

Experimental Investigation on the Pressure Propagation Mechanism of Tight Reservoirs

Jing Sun^{1,2,3,*}, Dehua Liu^{1,2,3}, Xiang Zhu^{1,2,3}, Wenjun Huang^{1,2,3} and Liang Cheng^{1,2,3}

¹Yangtze University, Petroleum Engineering College, Wuhan, China

²Hubei Cooperative Innovation Center of Unconventional Oil and Gas, Wuhan, China

³Hubei Shale Gas Development Engineering Technology Research Center, Wuhan, China

*Corresponding Author: Jing Sun. Email: sunjing_email@163.com

Received: 04 September 2019; Accepted: 07 January 2020

Abstract: Low permeability tight sandstone reservoirs have a high filtrational resistance and a very low fluid flow rate. As a result, the propagation speed of the formation pressure is low and fluid flow behaves as a non-Darcy flow, which typically displays a highly non-linear behavior. In this paper, the characteristics and mechanism of pressure propagation in this kind of reservoir are revealed through a laboratory pressure propagation experiment and through data from an actual tight reservoir development. The main performance mechanism is as follows: A new pressure cage concept is proposed based on the pressure variation characteristics of the laboratory experiments. There are two methods of energy propagation in the actual water injection process: one is that energy is transmitted to the deep reservoir by the fluid flowing through the reservoir, and the other is that energy is transmitted by the elasticity of the reservoir. For one injection well model and one production well model, the pressure distribution curve between the injection and production wells, as calculated by the theoretical method, has three section types, and they show an oblique “S” shape with a straight middle section. However, the actual pressure distribution curve is nonlinear, with an obvious pressure advance at the front. After the injection pressure increases to a certain level, the curve shape is an oblique and reversed “S” shape. Based on the research, this paper explains the deep-seated reasons for the difference in pressure distribution and proposes that it is an effective way to develop low permeability tight reservoirs using the water injection supplement energy method.

Keywords: Low permeability tight reservoir; pressure propagation; pressure cage; formation energy

1 Introduction

Propagation speed occurs due to low permeability tight sandstone reservoirs having a low permeability, a high seepage resistance and a very low fluid flow rate. Formation pressure is low, and fluid flow belongs to non-Darcy flow, which is a nonlinear flow. Pressure propagation occurs relatively fast near injection wells and production wells but occurs very slowly far away from production wells. In the actual production process, it is difficult to inject water into a low permeability oilfield without a fracture system. Oil



This work is licensed under a Creative Commons Attribution 4.0 International License, which permits unrestricted use, distribution, and reproduction in any medium, provided the original work is properly cited.

production mainly depends on formation energy in the process of oilfield development. When formation pressure drops to a certain extent, the productivity of oil wells is poor. It is necessary to supplement formation energy with water injection to continue production and improve oil recovery. In this way, a correct understanding of the law of pressure propagation plays an important role in improving the development effect of tight sandstone reservoirs.

The pressure propagation law of a low permeability reservoir is mainly studied from two aspects: pressure distribution and pressure propagation. The pressure distribution can be obtained by establishing the percolation model of a low permeability reservoir and by solving it, while the pressure propagation can be described by the influence radius [1]. Generally, the shut-in recovery curve, MBH method, MDH method, Dietz method and extended Muskat method are used to determine formation pressure overseas [2–4]. All these data must be able to shut favourably for well testing. Conventional methods are not applicable to low permeability oilfields because of slow pressure propagation and long pressure recovery time. For the influence radius, and different from Darcy seepage in the high permeability reservoir, there is a flow area radius for non-Darcy seepage in infinite formation, which is directly proportional to the production pressure and inversely proportional to the starting pressure gradient. Some scholars have further found that in the three seepage modes of plane parallel seepage, plane radial seepage and spherical centripetal seepage, the time required for the same distance of pressure wave propagation for the plane parallel seepage is twice that of the plane radial seepage, and the plane radial seepage is 1.5 times that of the spherical centripetal seepage [5–7]. Many scholars have studied the pressure propagation law in low permeability oilfields. Most of the studies are based on unstable seepage flow to establish pressure transfer equations to calculate and analyse the pressure distribution [8–20]. Some scholars consider the starting pressure and stress sensitivity to analyse the pressure propagation and test pressure distribution through a one-dimensional core flow experiment [21–23]. They believe that the starting pressure gradient and stress sensitivity have a greater influence on the pressure propagation. Some scholars also reveal the law of pressure wave propagation and its influence on productivity in low permeability reservoirs through numerical simulation technology [24]. Through calculations or experiments, some scholars also believe that the pressure blocking coefficient and medium deformation will affect productivity [25–27]. However, these results do not fully explain the pressure propagation characteristics, pressure propagation speed and their differences in different interwell locations of low permeability reservoirs. Additionally, the guiding role of the pressure propagation characteristics for actual production is not definitive. In this paper, a one-dimensional flow model is established using actual low permeability tight reservoir cores. To analyse the pressure propagation process, a number of measuring points are set between the entrance and the exit end of the long cores to monitor the pressure change at different locations. The pressure change characteristics are different between the experimental results and the theoretical calculation. At the same time, the effect of pressure propagation characteristics in low permeability reservoirs on oil well production is illustrated by combining a theoretical model and production data.

2 Experimental Study

Core experiments are an important way to study the migration law of oil and gas. Core experiments are helpful for understanding the seepage mechanism of oil and gas migration in special pore media with low permeability and tight reservoirs. Additionally, core experiments have good guidance and reference functions for the scientific and efficient development of low permeability and tight reservoirs. The cores used in conventional core physical simulation experiments are relatively short, usually only 5–8 cm. The end effect of the sample is notable in that the results cannot reflect the pressure propagation characteristics inside the core in the process of seepage. This experimental study used a 96.5 cm long core combination and a multiple pressure point seepage simulation system to overcome the end effect produced by short core experiments. The pressure dynamic propagation characteristics of low permeability and tight reservoir cores during single phase seepage and constant pressure of water flooding processes were studied, and these conditions truly reflected the seepage characteristics of low

permeability and tight reservoirs. Considering the actual production of low permeability and tight reservoirs, the pressure propagation law in the process of the water flooding and depletion development was simulated, and the exit end pressure of the long cores was set to atmospheric pressure and formation pressure.

The cores of this experiment were taken from a low permeability oilfield A and tight reservoir B. The cores were spliced into long cores of 96.54 cm and 90.16 cm. The weighted average permeability was 11.51 mD and 6.77 mD. The pressure distribution characteristics were tested by using a multi-point pressure measurement system. The production modes in the experiment were constant pressure displacement, constant speed displacement and depleting development, and the exit end pressure of the long cores was set to atmospheric pressure and bottom hole flow pressure.

2.1 Pressure Propagation Characteristics under Constant Pressure Displacement

Two experiments under constant pressure displacement were designed: one group with an entrance end pressure of 20 MPa and an atmospheric exit end pressure; the other group with an entrance end pressure of 30.5 MPa and an exit end pressure of 27.5 MPa. The pressure data of different measuring points at different times were measured every 5 min. Representative data were selected, and the pressure distribution along the long cores was plotted and analysed. Figs. 1 and 2 show the pressure testing data of each pressure measuring point at the different injection times under the entrance end pressure of atmospheric pressure and 27.5 MPa.

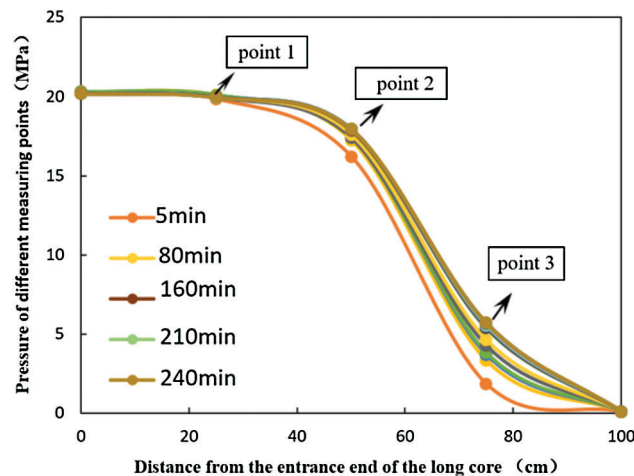


Figure 1: Pressure distribution curves along the core under constant pressure displacement (the exit pressure is at atmospheric pressure)

Figs. 1 and 2 show that the pressure distribution along the long core is nonlinear. With increasing cumulative injection time, the pressure drop from the exit end of the long core gradually propagates to the entrance. According to the experimental data, the following characteristics can be revealed:

1. Different pressure measuring points reflect that the changes in pressure vary by the distance from the entrance end. The farther the position is away from the entrance end, the faster the pressure decreases; the closer the position is to the entrance end, the slower the pressure decreases. This indicates that the pressure propagation from the exit end to the entrance end is slowed down gradually.
2. Fig. 1 shows that when the cumulative injection time is 240 min and the injection pore volume multiple reaches 0.16 PV, the pressure at pressure measuring point 1 reaches 19.96 MPa, which is equal to the pressure at the inlet.

3. The pressure gradient near the entrance is the smallest, the middle pressure gradient is the largest, and the pressure near the exit decreases. The pressure at point 2 is the pressure inflection point, after which the regional pressure drops rapidly.
4. Comparing the pressure propagation velocities of different pressure systems in Figs. 1 and 2, the exit end of high pressure and the exit end of low pressure have the same characteristics of pressure conduction. The pressure propagation velocity of the experiment with a large pressure difference is greater than that with a small pressure difference.

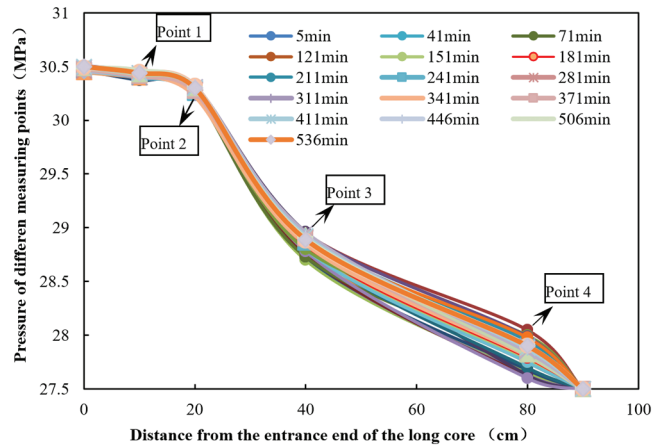


Figure 2: Pressure distribution curves along the core under constant pressure displacement (the entrance pressure is at 27.5 MPa)

2.2 Pressure Propagation Characteristics under Constant Speed Displacement

Two experiments under constant speed displacement were designed: one group with an entrance end pressure of 20 MPa and an atmospheric exit end pressure; the other group with an entrance end pressure of 30.5 MPa and an exit end pressure of 27.5 MPa. The pressure data of different measuring points at different times were measured every 5 min. Representative data were selected, and the pressure distribution along the cores was plotted and analysed. Figs. 3 and 4 show the pressure testing data of

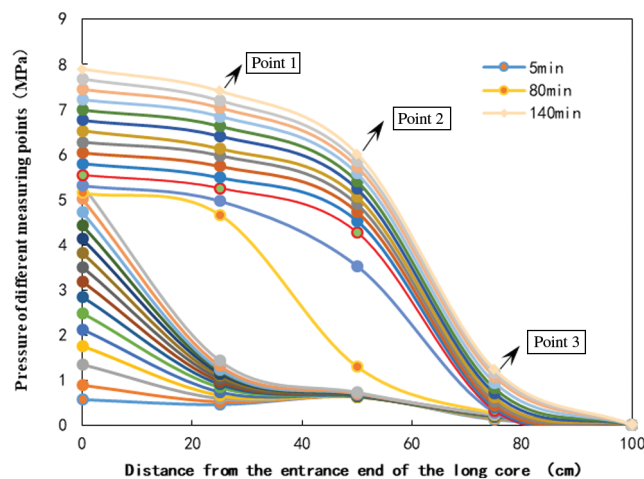


Figure 3: Pressure distribution curves of each measuring point under constant speed displacement (the entrance pressure is at atmospheric pressure)

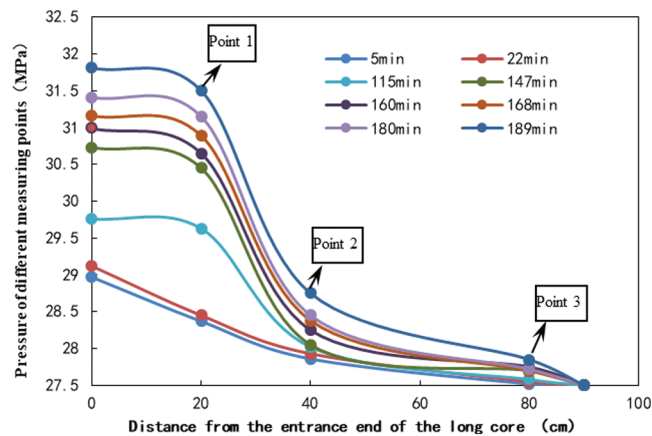


Figure 4: Pressure distribution curves of each measuring point under constant speed displacement (the entrance pressure is at 27.5 MPa)

each pressure measuring point at different injection times under the entrance end pressure of atmospheric pressure and 27.5 MPa.

The graphs shown in Figs. 3 and 4 demonstrate the pressure variation characteristics at each measuring point during constant speed displacement, and the results are as follows:

1. After the pressure wave reaches the measuring points, the pressure at each measuring point begins to increase. The pressure increases quickly in the initial stage and then slows down in the later stage, which indicates the nonlinearity characteristics of the pressure distribution.
2. The closer the position distance is from the entrance end, the faster the pressure increases. The slower the pressure increases at the position closer to the exit end, which indicates that the position is closer to the exit, the faster the pressure propagates. That is, the velocity of pressure propagation in the entrance and exit ends are faster than that in the intermediate part of the core.
3. According to the pressure distribution along the core, there is a pressure inflection point in the process of pressure propagation. The pressure gradient of the inflection point along the exit direction is larger, while the pressure gradient of the inflection point along the entrance direction is smaller.
4. The characteristics of pressure conduction with high pressure at the exit end are similar to those with low pressure at the exit end under constant speed displacement. Pressure propagation can be divided into two stages: ① Pressure accumulation stage: At this time, the pressure propagates slowly, and the injection system is in the energy accumulation stage. As shown in Fig. 3, when the cumulative injection time does not exceed 75 minutes, the pressure value at pressure measuring point 1 is small. ② The rapid release stage of pressure propagation: When the pressure accumulates to a certain extent, the pressure releases rapidly. As shown in Fig. 3, when the cumulative injection time exceeds 75 minutes, the pressure value at pressure measuring point 1 increases rapidly, and the propagation speed is the highest. The injection pressure of the whole injection system has an obvious first accumulation stage and then a release process. As shown in Fig. 3, under constant speed displacement, the pressure accumulates at the entrance for a long time until the entrance pressure increases to 5 MPa. After the pressure exceeds 5 MPa, the pressure begins to release and spread rapidly. That is, there is a pressure accumulation process in the initial stage of water injection in the low permeability or tight reservoir, which needs to maintain a certain injection time to achieve the effect of energy transmission and to complement recovery.

2.3 Pressure Distribution Characteristics under Depletion Development

Two experiments under depletion development were designed: one group with an entrance end pressure of 20 MPa and an atmospheric exit end pressure; the other group with an entrance end pressure of 30.5 MPa and an exit end pressure of 27.5 MPa. The pressure data of different measuring points at different times were measured every 5 minutes. Representative data were selected, and the pressure distribution along the core was plotted and analysed. Figs. 5 and 6 show the pressure testing data of each pressure measuring point at different injection times under the entrance end pressure of atmospheric pressure and 27.5 MPa.

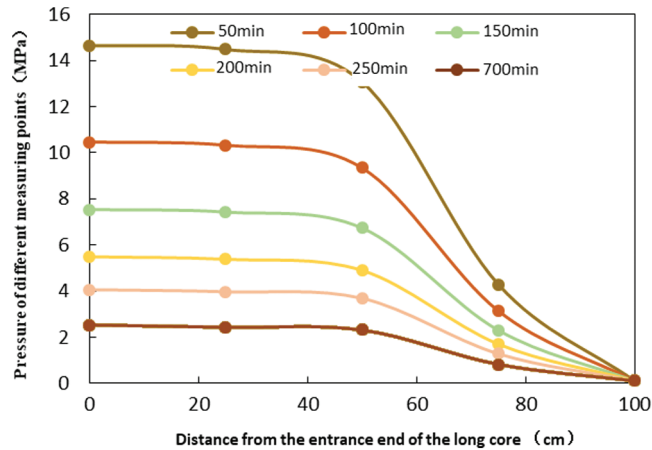


Figure 5: Pressure distribution curves of each measuring point under depletion development (the outlet backpressure is at atmospheric pressure)

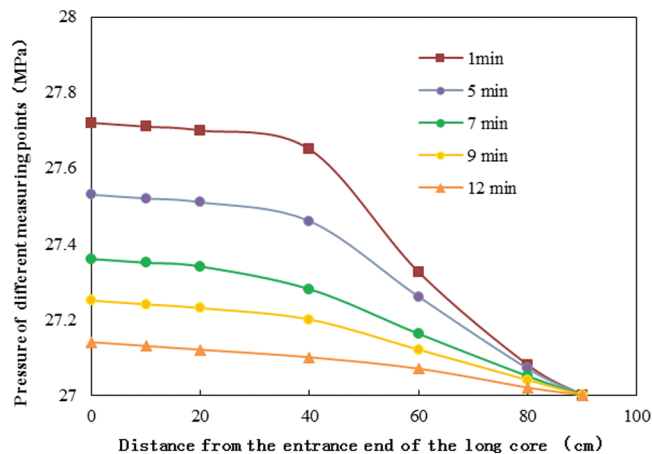


Figure 6: Pressure distribution curves of each measuring point under depletion development (the pressure of the entrance is 27.5 MPa)

The graphs shown in Figs. 5 and 6 demonstrate the pressure variation characteristics at each measuring point during depletion development, and the results are as follows:

1. Similar to the depletion development pressure drop process, the pressure at each point begins to decrease when the experiment starts. The closer the injection distance is from the entrance end, the faster the pressure decreases.
2. The pressure drop rate along the core is fast at the initial stage and decreases slowly as time proceeds.

3. During depletion development, the exit end of high pressure and the exit end of low pressure have similar characteristics of pressure conduction. As the pressure curve revealed above from the central point to the outlet area, the pressure has an accelerated downward trend.

3 Comparison of the Experimental Test Pressure Distribution and Predicted Pressure Propagation Law

There are mature theoretical prediction methods for the pressure distribution law of depletion development and for the supply of energy development. Based on the experimental results, the difference between the pressure distribution characteristics of the experimental test and the theoretical prediction is further analysed.

3.1 Mechanism of Formation Pressure Propagation in a Low Permeability Reservoir

Formation pressure reflects the rich degree of formation energy, and oil well production is a process of formation energy release. One of the main purposes of water injection is to supplement the formation energy. There is a difference between the supplement formation energy and release of formation energy. The release of the formation energy results in the continuous production of the well, and the fluid flowing is the energy release process. Generally, the production of oil wells depends on the release rate. After the well opens, the formation fluid flow mainly depends on the elastic energy of the formation. The elastic energy of the formation release is shown in the figure below.

Elastic energy mainly includes two kinds: rock elastic energy (as shown in Fig. 7) and fluid elastic energy (as shown in Fig. 8). Both the rock and the saturated fluid are compressible, and rock and fluid produce elastic forces during the oil and gas flow processes. When the formation pressure drops, the pressure difference between the overburden pressure and the formation pressure increases, the rocks are more closely arranged, and the pore volume decreases. The elastic energy of the rock tends the fluid towards the bottom of the well, as shown in Fig. 7. When the formation pressure drops, the fluid volume expands. The elasticity of the fluid causes the fluid to reach the bottom of the well, as shown in Fig. 8. With increasing production time, the elastic energy near the bottom of the well decreases gradually, forming a typical pressure drop funnel.

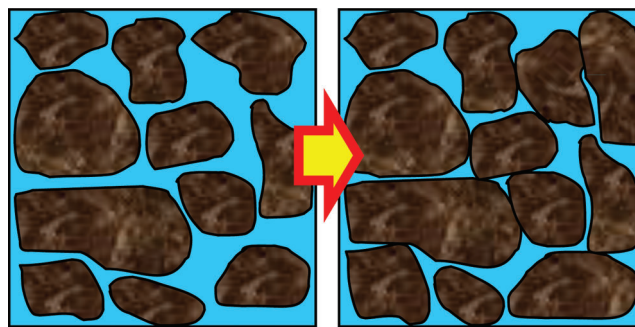


Figure 7: Rock releases elastic energy

3.2 Description of Pressure Distribution under Depletion Development

According to the description of the elastic unstable seepage law, the pressure distribution characteristics at any location in the reservoir under a closed boundary constant bottom hole pressure condition are shown in Fig. 9 [13].

As shown in Fig. 9, the formation pressure propagation under a closed boundary constant bottom hole pressure condition is divided into 2 stages. The first stage is that the pressure wave does not propagate to the

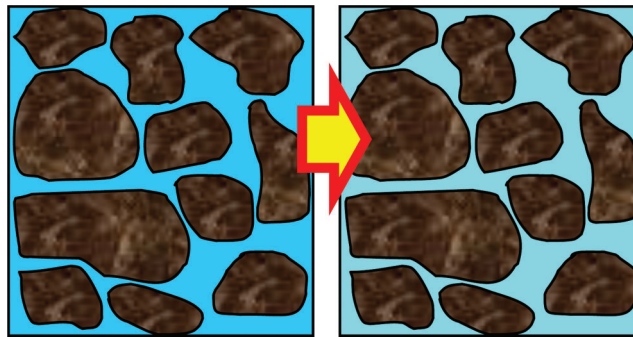


Figure 8: Fluid releases elastic energy

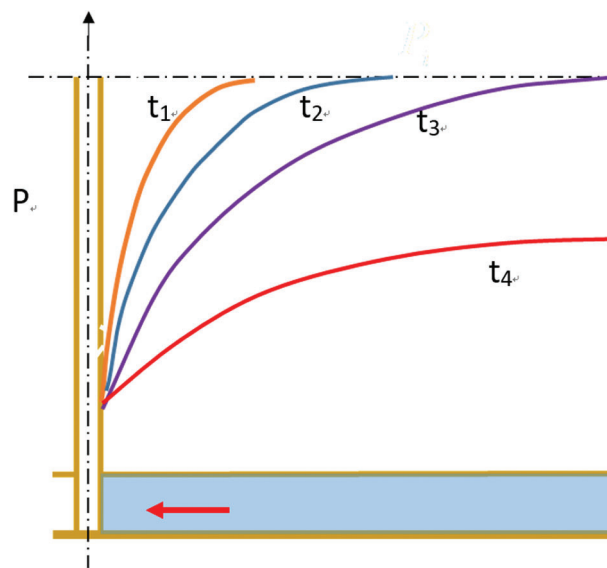


Figure 9: Pressure distribution characteristic curves at any location in the reservoir under a closed boundary constant bottom hole pressure condition

boundary, and the second stage is that the pressure wave propagates to the boundary. From the moment the first stage starts, the pressure drops continue to deepen at anywhere in the layer except at the well point, and the scope of the pressure drop funnel continues to expand. When the pressure wave propagates to the boundary, the boundary pressure decreases continuously because there is no external energy to supplement the boundary pressure until the pressure at any location in the formation equals the bottom hole pressure. The pressure distribution curve during the pressure propagation process at each stage is a standard nonlinear upper convex curve.

3.3 Description of Pressure Distribution between Two Wells: One for Injecting and the Other for Producing

Because of the rapid decrease in formation pressure during the development of low permeability or tight reservoirs, it is often necessary to inject a displacing medium to supplement the formation energy. The pressure formula of stable flow between one injection well and one production well is as follows [11]:

$$P = P_{iwf} - \frac{\alpha_1 \beta q}{2\pi h} \ln \frac{(L - r_w)r}{r_w(L - r)} - \frac{\alpha_2 \beta q}{2\pi h} \ln \left[\frac{2\pi h(L - r_w) + b\beta q}{2\pi h r_w + b\beta q} \frac{2\pi h r + b\beta q}{2\pi h(L - r) + b\beta q} \right] \quad (1)$$

where P is the pressure, Pa; B is the volume factor; q is the flow rate, m³/s; P_{iwf} is the injection well bottom hole flowing pressure, Pa; r_w is the well radius, m; r is the distance between the calculation point to the injection well, m; L is the distance from the injection well, m; h is the reservoir thickness, m; and α_1 , α_2 , and b are model parameter values.

Based on the core experimental data, the model parameter values α_1 , α_2 , and b are obtained, and the reservoir parameters are applied. Eq. (1) is used to calculate the distribution curve of position and pressure at different locations from the injection well, as shown in Fig. 10.

Fig. 10 shows the pressure distribution characteristics between the injection and production wells. The pressure at the injection end and the production end drops rapidly. The closer the distance from the injection or production well is, the greater the pressure gradient. With an interwell area of 30 m from the injection well and 30 m from the production well, the pressure clearly decreases. The pressure distribution in a conventional reservoir undergoes the same distribution rule. The pressure distribution feature is three-stage, and the pressure distribution between wells is linear. The shape of the pressure distribution curve near the bottom of the injection well is concave down, the shape near the bottom of the production well is upper convex, and the shape in the interwell is a straight line.

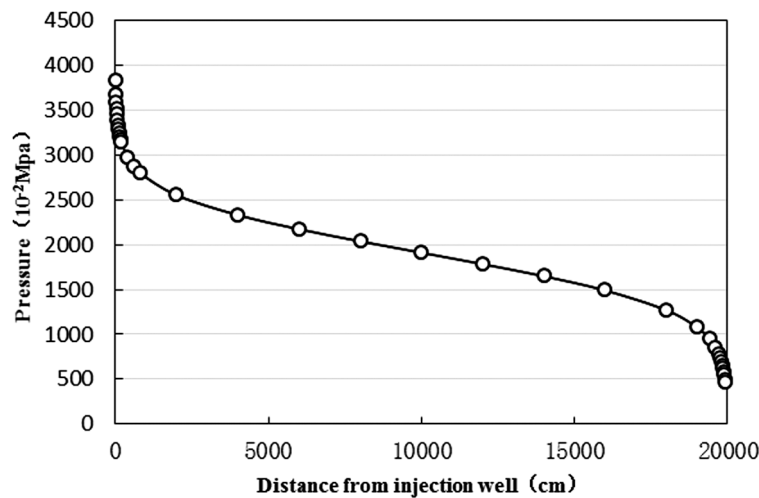


Figure 10: Typical curves for the pressure distribution between injection and production wells in the A oilfield low permeability reservoir

3.4 Differences between the Pressure Distribution by the Experimental Test and Pressure Distribution by the Theoretical Calculation

Figs. 9 and 10 describe the characteristics of the pressure change from the bottom hole to the supply boundary under the depleting development and under the supplementary energy development, respectively. Currently, this is the interwell pressure distribution described by the classical theory. The compressibility of reservoir rocks and fluids continues to change and the elastic energy release characteristics are not taken into account by the theoretical prediction method in the process of establishing an equation. Therefore, there are differences between the pressure distribution by the experimental test and the pressure distribution by the theoretical calculation.

3.4.1 Differences between the Pressure Distribution by the Experimental Test and Pressure Distribution by the Theoretical Calculation under Depleting Development

The theoretical pressure distribution curve from the production well to the closed boundary under a depleting development is shown in Fig. 9. The distribution curve of pressure from the supply boundary to the production bottom hole is upward convex; that is, the pressure drops rapidly near the production well. The experimental pressure distribution is different from the theoretical pressure distribution, as shown in Fig. 11. The experimental pressure is lower than the theoretical pressure in the area from the exit end to the centre. The distribution curve of pressure from the middle area to the production well bottom hole is concave down. The exit end of high pressure and the exit end of low pressure have a similar curve of pressure distribution under depletion development; that is, the same pressure distribution characteristics are shown. The difference between pressure distribution curves by the experimental test and theoretical calculation under depleting development is shown in Fig. 11.

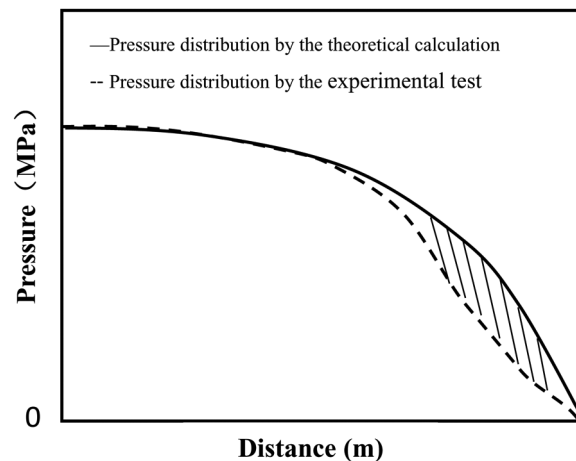


Figure 11: Pressure distribution curves by the experimental test and the theoretical calculation under depleting development

The reasons for this difference are as follows: according to the percolation theory, the seepage resistance near the bottom hole is the largest and pressure loss is fast, so the pressure near the bottom hole drops quickly. However, the compressibility coefficients of rock and fluids are regarded as a constant in the process of establishing a seepage equation without considering the change in compressibility coefficients of the reservoir rocks and fluids. When an actual well is put into production, the pressure decreases from the bottom of the well and spreads rapidly to the boundary. The transmitted energy comes from the release of the fluid and rock elastic energy. Because of the change in compressibility coefficients of rocks and fluids, the elastic energy has an accelerated release process in an area near the bottom of the well due to the large pressure difference. Therefore, the pressure drop rate in an area near the bottom of the well is faster than the theoretical calculation; that is, the actual pressure is lower than the theoretical calculation, and this result is generated in the experimental pressure distribution curve in Fig. 11.

3.4.2 Differences between the Pressure Distribution by the Experimental Test and Pressure Distribution by the Theoretical Calculation under Supplementary Energy Development

The pressure distribution between the injection and production wells, as calculated by the steady seepage formula of one injection well and one production well, has obvious three-stage characteristics, as shown in Fig. 10. The pressure near the bottom of injection-production wells decreases rapidly, with non-linear

characteristics. The pressure clearly descends in the interwell area, with linear characteristics. The shape of the complete curve is an oblique “S” shape. The curve is an inclined “S” shape.

However, the pressure distribution characteristics of the experimental test are significantly different from those of the theoretical calculations. The whole pressure characteristic of the experimental test under constant speed displacement is non-linear. The pressure distribution characteristics are divided into two stages, as shown in Figs. 3 and 4, respectively. In the first stage, the curve shape is an oblique “S” at the beginning of injection. In the second stage, after the injection pressure is increased to a certain level, the curve shape is an oblique and reversed “S” shape. When the injection pressure accumulates to a certain extent, the pressure drop at the injection end and the production end of the experimental test is different from that of the theoretical calculation. This shows that the pressure drops from the injection well to the middle area are relatively slower compared with the theoretical calculation, and the pressure drop is slower from the middle area to the production well. The pressure distribution difference between the experimental test and theoretical calculation under supplementary energy development is shown in Fig. 12.

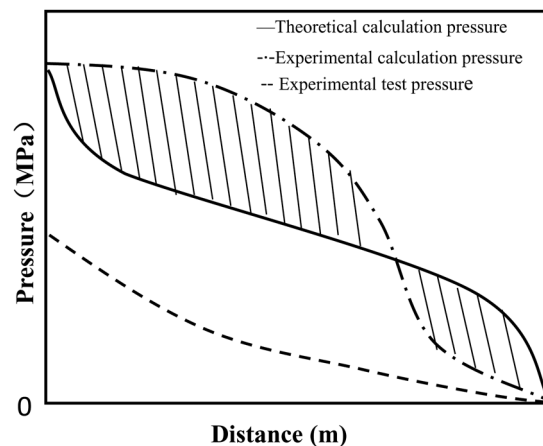


Figure 12: Interwell pressure distribution curves of the experimental and theoretical calculations under depleting development

The main reasons for this difference include the following:

1. The pressure drop from the injection well to the middle area is relatively slower compared with that of the theoretical calculation, and the main reason is that the release of rock and fluid elastic energy expansion accelerates the fluid flow and pressure propagation in the area near the production well bore. The decrease in pressure of the experimental test in the area near the bottom of the well is faster than that of the theoretical calculation. That is, because of the large pressure difference at the experimental exit end or the actual production bottom hole, the energy release is fast, and the phenomenon of accelerated decline occurs. However, the elastic compression coefficient considered in the theoretical calculation is treated as a constant, without considering the dynamic change in the compression coefficient of pressure release with pressure.
2. For the process of starting production and injection, the pressure drop at the injection end is gentle because the pressure transmission at the production end has not yet arrived via spreading. After injection for a period of time, a certain amount of energy accumulated at the injection end starts to propagate towards the outlet, and the pressure drop from the injection end to the front of the pressure step becomes stable.
3. Since the energy at the injection end accumulates and then propagates, a significant pressure step leading edge appears. A large pressure gradient appears outward at the leading edge of the pressure step, and this

indicates that the overall pressure distribution curve is nonlinear without a straight line segment in the middle. Therefore, the water injection process in a low permeability tight reservoir is a nonlinear flow.

For low permeability tight reservoirs, the velocity of the pressure reduction and outward propagation in the production bottom hole during development is faster than the theoretical predictions. The key ideas for actual production is as follows: the pressure of the injection well ends increase to a certain extent during the production process, and the pressure accelerates the propagation. Therefore, it is necessary to keep the water injection wells filled with enough water. The production bottom hole pressure decreases faster than the theoretical prediction, and the production of oil wells decreases rapidly. Therefore, it is important to determine the reasonable drawdown pressure and liquid producing capacity to maintain stable production or decrease the decline rate. It is necessary to avoid the phenomenon of enlarging the differential pressure production for actual production scenarios, which results in a decrease in pressure and a bottom hole liquid supply deficiency.

3.4.3 Proposal of the “Pressure Cage” Concept

When a constant velocity is injected, the pressure distribution curve appears in two forms. Its practical physical meaning is to supplement the formation energy at the beginning of fluid injection. Because of low permeability and high seepage resistance, it is difficult for pressure to diffuse outward. However, the injection pressure increases to a certain extent, as in Figs. 2 and 3 at 5 MPa, and the pressure begins to diffuse outward. The pressure diffusion mechanism can be divided into two forms. One is that fluid flow leads to pressure diffusion, which supplements formation energy. Second, the energy is transferred by elastic medium, and the injected energy gathers to a certain extent and then propagates outward through the elastic medium. Similarly, the energy of production wells can be supplemented, and at this time, the pressure distribution curve has an anti-S shape.

In the injection experiment, the pressure at the injection end accumulates to form a high pressure area, which is defined as a pressure cage. For the actual water injection well, its physical meaning is that with the increasing of the cumulative injection amount at the injection end, the accumulated energy gradually spreads out through the fluid and elastic medium, forming a high-pressure area, which is called pressure cage. Taking the injection well as the centre, the circular high-pressure zone is formed within the leading edge of the pressure step with the water injection well as the centre. The pressure profile between injection and production wells can be regarded as a pressure step near the injection wells, as shown in Figs. 1 and 2, between pressure point 2 and the injection end. The guiding effect of pressure cage on the actual production of low-permeability oilfield is as follows: It is difficult to inject water into low-permeability oilfield, and it is easy to fail to inject water. But if we keep water injection, the injected energy can be transferred by elastic medium. So, the energy can be supplemented, and enough production pressure difference can be maintained to maintain production well production. However, in the actual oilfield development process, the formation energy declines rapidly, and the recovery degree is low and completely dependent on the formation energy; thus, water injection is necessary for supplement formation energy. The existence of a pressure cage tells us that water injection can supplement formation energy. It is not necessary to pursue the water drive effect and water breakthrough to understand that energy is replenished. The transmission of energy by the elastic medium is also a good way to replenish energy, and the adequate injection volume must be maintained. The larger the pressure cage area is, the better the pressure propagation.

4 Application of Pressure Distribution of the Experimental Test

Based on the experimental data under constant speed displacement with the exit end pressure being atmospheric pressure, the velocity of pressure propagation and its application are analysed. As shown in Fig. 3, the pressure propagation characteristics are as follows: first, the pressure accumulates, and second,

the pressure releases rapidly; then, the velocity of pressure propagation slows down. The pressure propagation in different stages is analysed.

4.1 Calculation and Application of Pressure Accumulation Stage

Based on the experimental results under constant speed displacement with the exit end pressure at atmospheric pressure, when the ratio of cumulative injection volume to core pore volume is approximately 0.1, the pressure starts to release rapidly. Take reservoir A as an example to calculate the pressure accumulation time. The pattern of the reservoir is a five-spot pattern with 300 m well spacing. The reservoir thickness is 2 m, the porosity is 16.2%, and the daily injection volume is 20 m³. According to the ratio of cumulative injection volume to core pore volume, which is approximately 0.1, we can calculate the cumulative time for pressure accumulation. The result of the cumulative time is 110 days. The pressure begins to propagate rapidly when the cumulative injection time reaches 110 days.

4.2 Calculation and Application of Rapid Release Pressure Velocity after Pressure Accumulation

Based on the experimental results under constant speed displacement with the exit end pressure at atmospheric pressure, the curve of the increasing pressure velocity of each measuring point of the long core is plotted in Fig. 13. We can calculate the rapid release pressure velocity after pressure accumulation.

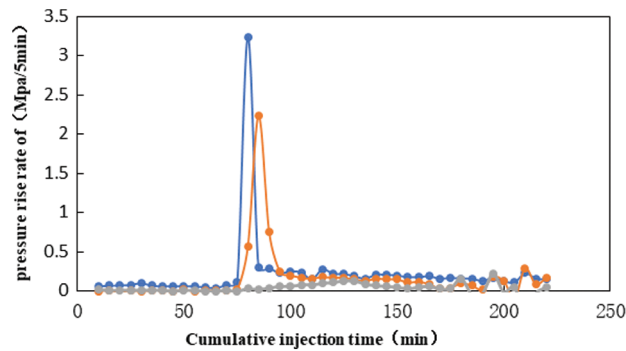


Figure 13: Pressure rise rate curves of each measuring point

According to the pressure rise rate curves of each measuring point, when the cumulative injection time is 80 min, the value of the pressure rise rate at pressure measuring point 1 is the highest. When the cumulative injection time is 85 min, the value of the pressure rise rate at pressure measuring point 2 is the highest. The distance from pressure measuring point 1 to pressure measuring point 2 is 25 cm. The time it takes for the pressure to propagate from pressure measuring point 1 to pressure measuring point 2 is 5 min. Therefore, we can calculate that the rapid release pressure velocity after pressure accumulation is 5 cm/min. This pressure velocity is the pressure rapid release velocity under constant speed displacement after pressure accumulation. After the pressure spreads rapidly, the pressure propagation returns to a slow rate again.

4.3 Calculation of Time of Injected Water Energy Propagation to the Bottom of the Production Well

The velocity of pressure propagation is related to the real rate of flow under constant speed displacement. Assuming that the leading edge propulsion speed velocity V_f is linearly related to the real rate of flow v , the relationship can be expressed by the following equation:

$$V_f = k \cdot v \quad (2)$$

where k can be obtained according to the experimental results of constant displacement, and the range of k is from 2 to 10.

When the seepage mode is plane radial flow, the real rate of flow can be described as follows:

$$v = \frac{q}{2\pi rh\phi} \quad (3)$$

The pressure leading edge propulsion model of the plane radial flow is established. Suppose that the distance between the production well and injection well is L , the time of the pressure transfer from the injection wells is t , and the time for the pressure leading edge conducting to any position from the injection wells (r) can be calculated by the following equation:

$$dt = \frac{dr}{V_f} \quad (4)$$

Substituting Eqs. (2) and (3) into Eq. (4) gives:

$$\int_0^t dt = \int_r^L \frac{2\pi rh\phi}{kq} dr \quad (5)$$

Integrating Eq. (5) gives:

$$t = \frac{\pi h\phi}{kq} (L^2 - r^2) \quad (6)$$

where q is the injection rate, m^3/d ; ϕ is the porosity; t is the time of the pressure leading edge conducting to any position from injection wells (r), d ; L is the distance between the production wells and water wells, m ; h is the reservoir thickness, m ; and k is the coefficient between the leading edge propulsion velocity (V_f) and the real rate of flow (v), where the range of k is from 2 to 10.

Taking reservoir A as an example where the value of k is 5. According to the experimental results, we can determine that the time of injected energy propagating to the bottom of the production well is 345 days. That is, the response time of oil wells is 345 days.

The model assumes that the leading edge propulsion speed velocity (V_f) is linearly related to the real rate of flow (v), and the relationship is $V_f = f(v)$. The experimental data can also be used to fit the relationship curve between the pressure leading edge propagation velocity and the real rate of flow to improve the mathematical model above. The simplified model establishes the relationship between time, water injection volume and pressure propagation distance, which can be used to analyse the rationality of advanced water injection, production allocation and well spacing optimization of reservoirs.

5 Discussion

The experimental results and the law of pressure propagation can effectively guide the actual development of the reservoir:

1. Water injection is the most economical and effective way to replenish formation energy. During the injection process, the formation energy transmission can be transmitted to the production well through reservoir rocks and fluids. Keeping a reasonable and adequate injection rate is the basis for ensuring the output of oil wells. In the actual injection process, there will be problems such as poor injection capacity and high injection pressure. One way that injection energy can spread to the bottom of production well is through the elastic medium of the reservoir through cyclic waterflooding. For the

formation of cyclic waterflooding, when the high ratio of the stop injection is 2, the degree of reserve recovery is highest. The second way is to generate hydrodynamic waves to change the physical properties of the reservoir by pulse water injection and accelerate the energy propagation through the reservoir.

2. When the production well is put into operation, the output of the well is due to the contribution of fluid and rock elastic energy. For energy-rich reservoirs or differential pressure amplification, oil production can be increased in a short time. According to the analysis of pressure propagation characteristics in the front, the decline of formation pressure near production wells is accompanied by an accelerated decline in well production. That is, when the fluid propagates energy, the elastic medium also releases the elastic energy by expansion, and the formation pressure is accelerated to decrease. If the pressure difference is too large, the release of elastic energy of the elastic shale is too fast, and a pressure-sensitive effect will appear, which results in a rapid decline in oil production or even no oil production. In the actual production process, it is necessary to determine the reasonable production pressure difference and liquid producing capacity of oil wells according to the formation pressure level. According to the experimental analysis of the pressure propagation law, it is better to control the pressure difference between 2 and 5 MPa. If the pressure difference exceeds 5 MPa, the production wells will accelerate the energy transmission, that is, the pressure-sensitive effect will appear.

6 Conclusion

This paper reveals the characteristics and mechanisms of pressure propagation in low permeability reservoirs through laboratory pressure propagation experiments and actual development data and draws the following conclusions.

1. There are two methods of energy transmission in the actual water injection process: one is through fluid flow to the deep reservoir, and the other is through the elastic transmission of the reservoir itself. The layer energy performance first accumulates and then propagates at the bottom of the water injection well, and rapid acceleration characteristics appear at the bottom of the production well.
2. For low permeability tight reservoir waterflooding, a new pressure cage concept is proposed based on the characteristics of pressure variation in laboratory tests. That is, the pressure first gathers at the bottom of the water injection well and then begins to propagate outward after reaching a critical value. When the formation pressure is low, the formation pressure begins to propagate outward after increasing to 5 MPa. When the formation pressure is high, the formation pressure rapidly spreads outward after increasing to 2 MPa.
3. Based on the research, it is proposed that water injection and replenishing energy in low permeability tight reservoirs are the basis for effective development. Combined with the actual low permeability reservoir development, suggestions for improving the water injection effect are given. The pressure propagation velocity characterization equation is given in combination with the experiment to clarify the actual injection time of the actual reservoir.

Funding Statement: This work was supported by the National Science and Technology Major Project Fueling Shale Gas Development Demonstration Project [grant number 2016ZX05060]; the Science and Technology Innovation Foundation of CNPC [grant number 2016D-5007-0208].

Conflicts of Interest: The authors declare that they have no conflicts of interest to report regarding the present study.

References

1. Zhang, L. (2009). *Study on pressure propagation law of low permeability reservoir*. Beijing: China University of Petroleum.

2. Matthews, C. S., Brons, F., Hazebroek, P. (1954). A method for determination of average pressure in a boundary reservoir. *Trans AIME*, 201, 182–191.
3. Miller, C. C., Dyes, A. B., Hutchinson, C. A. Jr. (1950). The estimation of permeability and reservoir pressure from bottom-hole pressure build-up characteristics. *Trane, AIME*, 2(4), 91–104.
4. Dietz, D. N. (1965). Determination of average reservoir pressure from build-up surveys. *Journal of Petroleum Technology*, 17(8), 955–959. DOI 10.2118/1156-PA.
5. Ge, J. L. (1982). *Seepage mechanics of oil and gas reservoir*. pp. 108–110. Beijing: Petroleum Industry Press.
6. Xiao, L. C., Zhen, L., Zhen, Y. (2000). Study on non Darcy percolation characteristics of ultra-low permeability reservoir. *Petroleum Geology & Oilfield Development in Daqing*, 19(5), 27–30.
7. Prats, M. (1961). Effect of vertical fractures on reservoir behavior-incompressible fluids case. *Society of Petroleum Engineers Journal*, 1(2), 105–118. DOI 10.2118/1575-G.
8. Zhu, S. J. (2002). The law of pressure spread in different flow states. *Xinjiang Petroleum Geology*, 23(6), 522–523.
9. Li, A. F., Chen, M. Q., Song, H. P. (2016). Study on pressure propagation in low permeability reservoirs. *Science Technology and Engineering*, 16(2), 47–51.
10. Ji, B. Y., He, Y. F. (2011). Formation pressure distribution of a single well based on low-velocity non-Darcy flow. *Acta Petrolei Sinica*, 32(3), 466–469.
11. Zhu, W. Y., Liu, J. Z., Song, H. Q. (2010). Calculation of effective startup degree of non-Darcy flow in low or ultra-low permeability reservoirs. *Acta Petrolei Sinica*, 31(3), 452–457.
12. Li, X. Y. (2016). Study on pressure distribution of fractured low permeability reservoirs with dynamic starting pressure gradient. *Liaoning Chemical Industry*, 10(8), 1305–1307.
13. Liu, H. L., Wang, G., Wu, S. H. (2016). A study on pressure transmission of unsteady fluid flow in banded fault block reservoir. *Journal of Southwest Petroleum University (Science & Technology Edition)*, 38(5), 135–142.
14. Liu, H. L. (2016). Dynamic analysis of unsteady seepage pressure in low permeability rectangular reservoirs. *Journal of Anhui University of Science and Technology (Natural Science)*, 36(1), 75–82.
15. Qiao, W., Wang, L. Q., Zhang, Z. G. (2012). Pressure wave propagation of fracturing well in ultralow permeability reservoir. *Xinjiang Petroleum Geology*, 17(8), 955–959.
16. Kucuk, F., Brigham, W. E. (1981). Unsteady-state water influx in elliptical and aniso-tropic reservoir/aquifer system. *Society of Petroleum Engineers Journal*, 21(3), 309–314. DOI 10.2118/8748-PA.
17. Zhu, W. Y., Qi, Q., Ma, Q. (2016). Unstable seepage modeling and pressure propagation of shale gas reservoirs. *Petroleum Exploration and Development*, 43(2), 261–267. DOI 10.1016/S1876-3804(16)30029-5.
18. An, S. P., Li, J., Yu, P. L. (2016). Pressure transient characteristics of hydraulically fractured horizontal wells in tight oil reservoirs. *Science Technology and Engineering*, 16(15), 84–91, 110.
19. Cinco, L. H., Milier, F. G. (1975). Unsteady-state pressure distribution created by a directionally drilled well. *Journal of Petroleum Technology*, 11(15), 1392–1400.
20. Jiang, R. Z. H., Shen, Z. Y., Cui, Y. Z. (2018). Dynamical characteristics of inclined well in dual medium low permeability reservoir. *Lithologic Reservoirs*, 30(6), 131–137.
21. Wu, D. F., Lu, X. B., Liu, Q. J. (2012). Pressure distribution in flooding of low permeability reservoirs. *Mechanics in Engineering*, 34(5), 27–31.
22. Ma, F. B., Ge, H. K., Wang, Y. (2015). Research of ultra-low permeability formation pressure propagation. *Science Technology and Engineering*, 15(9), 81–84.
23. Zhao, C. P., Yue, X. G. (2011). Long-core experimental study on advance water injection of extra-low permeability reservoir. *Journal of Southwest Petroleum University (Science & Technology Edition)*, 33(3), 9105–108, 197.
24. Li, F. Y., Hong, C. Q., Ren, C. Q. (2015). The propagation law of pressure wave in low permeability reservoir and its impact on production capacity. *Petrochemical Industry Application*, 4, 10–13.
25. Gao, S. S., Xiong, W., Liu, X. G. (2010). Current situation and new understanding of experimental study on gas percolation mechanism in low permeability sandstone gas reservoir. *Natural Gas Industry*, 30(1), 52–55.
26. Liu, N. Q. (2008). *Practical modern well test interpretation method (Fifth Edition)*. Beijing: Petroleum Industry Press.
27. Zhang, Y., Cheng, J. P., Fang, D. (2013). Discussion on pressure propagation calculation method based on non Darcy seepage. *China Petroleum and Chemical Standard and Quality*, 33(11), 253.